ADVANCED FUNCTIONAL MATERIALS
www.afm-journal.de

Plasmonic Particles that Hit Hypoxic Cells

Fulvio Ratto, Ewa Witort, Francesca Tatini, Sonia Centi, Lorenza Lazzeri, Fabrizio Carta, Matteo Lulli, Daniela Vullo, Franco Fusi, Claudiu T. Supuran, Andrea Scozzafava, Sergio Capaccioli, and Roberto Pini*

The use of gold nanorods as contrast agents for the optical hyperthermia of cancer is receiving ever more attention. However, their selective delivery to tumors still remains an outstanding problem. In most cases, the identification of suitable molecular targets is complicated by the lack of qualitative differences between healthy and cancer cells. The focus of prior work has mainly been on the cancer cells per se. Instead, here, the aim is moved to secondary fingerprints that arise in response to the cancer microenvironment. One common feature of tumors is a combination of poor oxygenation and high oxygen consumption, which generates hypoxia. Hypoxic cells need to switch to an anaerobic metabolism, which is accompanied by a multitude of molecular processes, including the expression of transmembrane isoforms of carbonic anhydrases. Here, gold nanorods are conjugated with selective inhibitors of these enzymes, in order to recognize and hit hypoxic cells. The cellular uptake, cytostatic activity and capacity to impart an optical sensitization of these particles is shown to display a strong dependence on environmental oxygenation.

1. Introduction

In recent years, the notion to combine near infrared (NIR) light and NIR contrast agents for biomedical applications has received much interest.[1–4] This combination profits from the low absorption and deep penetration of NIR light into biological tissue. Examples of applications include the photoacoustic imaging[5–8] and optical hyperthermia[1,4,7] of cancer. In this context, a critical issue remains the development of contrast agents with ideal biological profiles, high optical absorbance and the ability to target malignant cells. The use of novel particles such as gold nanorods,[1,2,8–11] nanoshells,[12,13] nanocages[5,14] and other shapes with plasmonic bands in the NIR window has aroused much hope, with a large number of preclinical and even a few clinical trials[15] underway. These particles exhibit excellent tolerability both in vitro and in vivo,[16–18] efficiency and stability of photothermal conversion and the potential to home into tumors.[5,18,19] The latter relies on a subtle interplay of different effects, requiring a thoughtful particle design. Coating of the particles with polyethylene glycol (PEG)[6,9,16,20–22] is a popular approach, since the PEG portion provides the appropriate steric hindrance and prevents flocculation and the detection from macrophages. As a consequence, the blood clearance of PEGylated particles becomes slower, thus playing in favor of their passive accumulation into tumors that exhibit enhanced permeability and retention (EPR).[23] This passive effect may be improved by the addition of ligands for molecular targets expressed on the plasmatic membranes of malignant cells.[19] Examples of ligands include antibodies,[1,8,12,24–31] aptamers,[32–34] peptides[19,35–37] and small molecules,[11,38,39] which may be combined for synergistic approaches.[40–42]

The molecular targets are usually taken among the fingerprints of a certain population of malignant cells per se. In general, their identification is a tremendous task, because the phenotypes of malignant cells may differ much from case to case and still resemble much those of normal cells in terms of biochemical diversity. In most of the recent literature, this choice falls on features that reflect the higher proliferation of neoplastic vs healthy cells, such as the epidermal growth factor receptors (EGFR),[1,12,19,24–26] the vascular endothelial growth factor receptors (VEGFR),[43] or the folate receptors.[11,38] However, these macromolecules belong to both malignant as well as normal cells and their expression only differs on a quantitative level. For instance, the density of EGFR is only about an order of magnitude higher in typical malignant EGFR-positive than in most normal cells.[44,45]

Dr. F. Ratto, Dr. F. Tatini, Dr. R. Pini
Institute of Applied Physics
National Research Council of Italy
via Madonna del Piano 10, 50019 Sesto Fiorentino, Italy
E-mail: f.ratto@ifac.cnr.it
Dr. E. Witort, Dr. S. Centi, L. Lazzeri, Dr. M. Lulli, Prof. F. Fusi, Prof. S. Capaccioli
Department of Experimental and Clinical Biomedical Sciences
University of Florence
Viale Morgagni 50, 50134 Florence, Italy
Dr. F. Carta, Dr. D. Vullo, Prof. A. Scozzafava
Department of Chemistry
University of Florence
Via della Lastruccia 3, 50019 Sesto Fiorentino, Italy
Prof. C. T. Supuran
Dept. of Neuroscience, Psychology
Drug Research and Child Health, Univ. of Florence
Viale Pieraccini 6, 50139 Florence, Italy

DOI: 10.1002/adfm.201402118

Rather than the single cells per se, more distinctive alternatives arise from the difference between neoplastic and healthy microenvironments. Peculiar consequences of the incoherent vascularization and high oxygen consumption of solid tumors are necrosis and hypoxia. The latter is a typical feature of aggressive tumors and correlates with a poor prognosis and metastatization.[46,47] Moreover, it is established that cancer is maintained by a certain population of stem cells that exhibit resistance to chemotherapeutics and require hypoxia.[48,49] Under conditions of low oxygenation, all cells make a metabolic switch from oxidative phosphorylation to anaerobic glycolysis, which generates acidic species, such as lactic acid. Meanwhile, a multitude of processes begin with the intent to preserve the intracellular pH from acidification.[50–54]

The most efficient system of physiological buffering is the hydration of carbon dioxide into carbonic acid, which is catalyzed by the metalloenzymes carbonic anhydrases (CAs).[55–64] Thus far, 16 different isoforms of CAs differing by catalytic activity, regulatory mechanism, cellular and tissue distribution[61,62] have been reported in humans. In particular, the expression of CAIX and, in some cases, CAXII was found to accompany the transformation from normal into malignant cells and promote cellular migration and metastatization.[62–71] Unlike all others, CAIX and CAXII are transmembrane isoforms and expose their catalytic cavities toward the extracellular environment.

In recent years, some of us began to investigate the role of CAIX in malignant cells and novel approaches for its selective inhibition.[69] In 2004, Svastova et al.[52] demonstrated the use of fluorescent compounds containing sulfonamides to inhibit CAIX and act as a potent anticancer drug. After that, various small molecules have been proposed as CA inhibitors (CAIs), including sulfonamides and their structural isosteres, such as sulfamates and sulfamides, coumarines and their mono/dithio derivatives.[72,73] Specificity for CAIX and CAXII is pursued by the addition of moieties that prevent the penetration of plasmatic membranes, thus avoiding the contact of these compounds with intracellular CAs.[74] This function has already been assigned to gold nanospheres as well.[75,76]

Here we build on all these developments and propose the use of derivatives of sulfonamides and gold nanorods as selective anticancer and NIR contrast agents. The notion to target tumor-associated CAs for the photoacoustic imaging and optical hyperthermia of cancer is a prime novelty. We expect that this combination may mark a step-change in the use of plasmonic particles in oncology, thanks to the correlation between cancer and hypoxia.

2. Results and Discussion

2.1. CAI-Conjugated Gold Nanorods

All details on the preparation of our particles are given in the Experimental Section.

Figure 1 displays a representative transmission electron micrograph of as-synthesized cetrimonium-terminated gold nanorods, prior to their PEGylation and modification with either of 2-methoxyethylamine, as a negative control that mimics the use of methoxylated PEG, or 4-(2-aminoethyl)benzenesulfonamide, as a model of sulfonamide-bearing CAI. These gold nanorods exhibit a smooth profile with little so-called dog-bone shapes,[77] aspect ratios of 4.3 ± 0.5 and effective radii of (9.8 ± 1.4) nm. Figure 1 also shows a comparison of the light extinction spectra of cetrimonium-terminated, CAI- and 2-methoxyethylamine-conjugated gold nanorods in aqueous suspensions. Their typical plasmonic bands did not change from sample to sample, which implies that particles did not aggregate upon modification.[2,26,78,79] Instead, we detected subtle variations of their electrokinetic potentials, in agreement with their manipulation and addition of their different portions. After PEGylation in an acetate buffer and modification in a MES buffer, the strong positive charge of cetrimonium-terminated gold nanorods[80] underwent inversion. For CAI- and 2-methoxyethylamine-conjugated particles in PBS, we found average values of (–8.1 ± 0.8) and (–13.5 ± 1.1) mV, respectively, both with std deviations as large as ≈14 mV. We anticipate that a fraction of particles with cationic profile is likely to undergo nonspecific interactions with the cellular membranes, as it has been discussed in the recent literature.[79,81,82] The number of functional CAI molecules per CAI-modified particle was estimated to be 200 ± 100, by the measurement of their catalytic activity (see Figure S1 in Supporting Information).

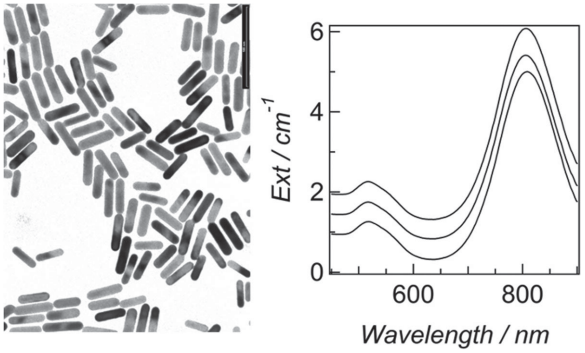

Figure 1. Left: 300 nm × 400 nm representative transmission electron micrograph of as-synthesized gold nanorods. Right: optical extinction spectra of cetrimonium-terminated, CAI- and 2-methoxyethylamine-conjugated particles in aqueous suspensions, respectively from bottom to top.

2.2. Particle Cytotoxicity

Particle cytotoxicity was first inspected in normoxia for two relevant models, that is, human HCT116 (HCT hereafter) colon colorectal carcinoma and human MDA-MB-231 (MDA hereafter) mammary adenocarcinoma cells. In essence, the MTT analysis in **Figure 2** reveals an absence of inhibition of mitochondrial activity after 24 h exposure to 2-methoxyethylamine- and CAI-labeled particles.

2.3. Particle Targeting In Vitro

Figure 3 shows a collection of optical micrographs of cells kept under different oxygenation levels and treated with different

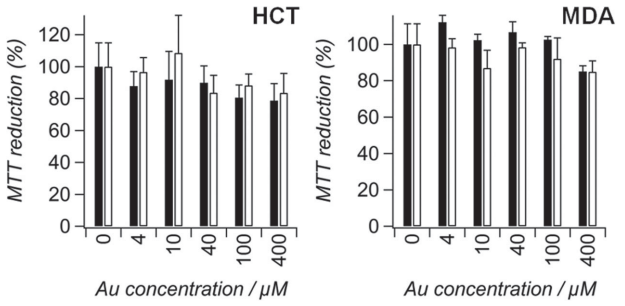

Figure 2. Percent of MTT reduction for HCT (left panel) or MDA (right panel) cells kept in normoxia and treated for 24 h with CAI- (black bars) or 2-methoxyethylamine- (white bars) terminated particles with different gold concentrations.

particles, which were stained by silver precipitation. On immediate visual inspection, silver enhancement reveals a clear preferential accumulation of gold nanorods for the combination of CAI-conjugation and hypoxic incubation both for the HCT and MDA cells. Instead, normoxia or the absence of CAIs were sufficient to avoid most of this accumulation.

This qualitative evidence is confirmed by the quantification presented in **Table 1**, which was retrieved from an inspection of cellular pellets by spectrophotometry and its numerical analysis (see the Experimental Section). For the sake of comprehensiveness, representative optical extinction spectra are reported in Supporting Information. The overlay of the experimental data with their numerical model shows a good agreement. All cellular pellets exhibited a good persistence of the pristine

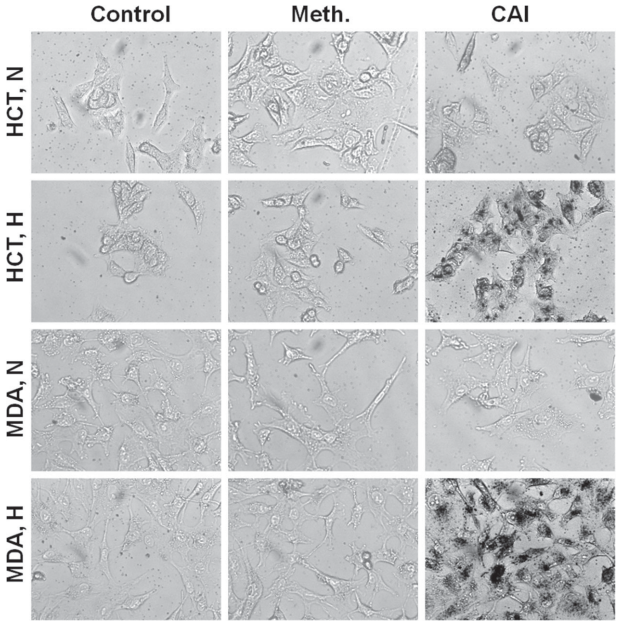

Figure 3. 350 μm × 250 μm optical micrographs of HCT or MDA cells in normoxia (N) or hypoxia (H), treated without particles (Control) or with 100 μM Au 2-methoxyethylamine- (Meth.) or CAI-terminated particles and finally stained with silver, which reveals the accumulation of metallic nuclei. Silver was left to interact for different times with the HCT or MDA cells (shorter for the HCT and longer for the MDA cells), which precludes their comparison.

Table 1. Average mass of gold per cells from a numerical deconvolution of the optical extinction spectra. HCT and MDA cells were grown under different levels of oxygenation, i.e., hypoxia (H) or normoxia (N), and treated with 100 μM Au particles with different modifications, i.e., CAIs, anti-CAIX antibodies or 2-methoxyethylamine (Meth.), over 24 h before the spectrophotometric inspection.

Cells	Oxygenation	Particles	pg Au per cell
HCT	H	CAI	1.8 ± 0.4
		Anti-CAIX	1.3 ± 0.3
		Meth.	0.1 ± 0.2
	N	CAI	0.3 ± 0.2
		Anti-CAIX	0.1 ± 0.2
		Meth.	0.1 ± 0.2
MDA	H	CAI	0.5 ± 0.2
		Anti-CAIX	0.4 ± 0.2
		Meth.	0.2 ± 0.2
	N	CAI	0.2 ± 0.2
		Anti-CAIX	0.2 ± 0.2
		Meth.	0.2 ± 0.2

plasmonic lineshape of the aqueous suspensions of gold nanorods, which implies that the particles retained most of their shape and individual response.[79] In practice, the values in the rightmost column of Table 1 scale with the weak growth of the optical density around 800 nm, as due to an accumulation of gold nanorods. So, the proportions of these values remain accurate, independent of the details of the numerical model, and may be read as a standard immunogold experiment.[12,24] Moreover, in some cases, we verified that their quantification is consistent with an elemental analysis, which is reported in Table S1 of Supporting Information.

Table 1 corroborates the specificity of CAI- and another positive model of anti-CAIX antibody-conjugated particles for hypoxic cells. In more detail, the contrast is found to be higher for HCT than MDA cells and probably also for CAI- than anti-CA9-modified particles. The former may suggest a higher turnover of transmembrane CAs in HCT than MDA cells, in our particular experimental conditions. The latter may be attributed to a combination of steric effects limiting both the payload and proper orientation of larger probes, such as antibodies, with misplaced amines available for the conjugation.[27,28] We anticipate that the absolute rates of CAI- and anti-CA9-conjugated particles per hypoxic HCT cells may be adequate for a useful sensitization to their optical hyperthermia.[83] The low affinity of particles conjugated with 2-methoxyethylamine both for normoxic and hypoxic cells derives from the efficiency of the PEGylation and demonstrates the role of CAIs or anti-CAIX antibodies in the cellular uptake. However, we notice the undesirable occurrence of nonspecific uptake of CAI-conjugated particles in normoxic HCT cells. We speculate that this effect may be ascribed to the residual cationic profile of 4-(2-aminoethyl) benzenesulfonamide,[84] shifting the electrokinetic potential of CAI-labeled particles by ≈+5 mV and thus favoring their cellular adhesion.[79,81,82] We envision that this nuisance may be removed by suitable engineering of different inhibitors taken

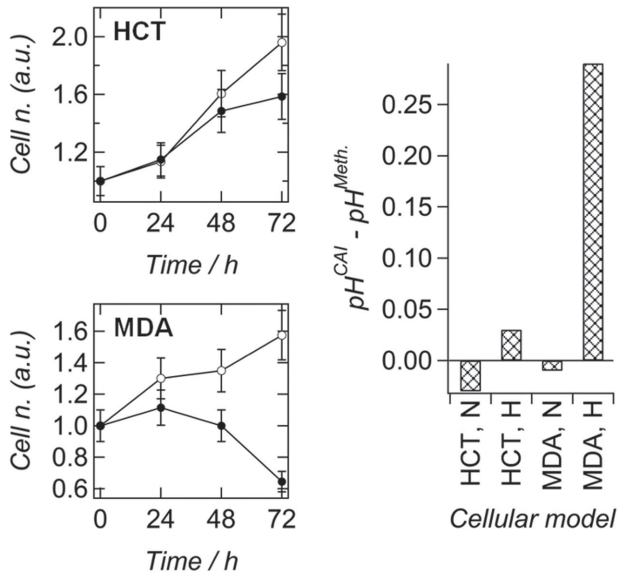

Figure 4. Left panels: relative counts of HCT or MDA cells incubated in hypoxia with 100 μM Au CAI- (black symbols) or 2-methoxyethylamine- (white symbols) terminated particles. Right panel: differential modulation of extracellular pH for HCT or MDA cells in normoxia (N) or hypoxia (H) and treated with CAI- and 2-methoxyethylamine- (Meth.) terminated particles.

from their pool of alternatives,[72,73] which will be the subject of future efforts.

2.4. Therapeutic Potential without an Optical Excitation

A time-lapse analysis of cellular proliferation in hypoxia is shown in **Figure 4** (panels on the left). 2-methoxyethylamine-modified particles were seen to be non cytotoxic in both cellular models even in hypoxia. Instead, the presence of CAIs induced a clear cytostatic effect that was fairly stronger for MDA than HCT cells. We found a severe inhibition of cellular proliferation, while the incidence of cellular death by apoptotic or necrotic events was comparable to that of control samples without particles. We note that this finding is in line with the effect observed after administration of CAIs alone.[69] Representative excerpts of time-lapse video-registrations are given as Supporting Information: HCT cells treated with 2-methoxyethylamine-conjugated particles in hypoxia, HCT cells treated with CAI-conjugated particles in hypoxia, MDA cells treated with 2-methoxyethylamine-conjugated particles in hypoxia, MDA cells treated with CAI-conjugated particles in hypoxia. The comparison between HCT and MDA cells suggests that the cytostatic effect seen in Figure 4 does not simply correlate with the accumulation of particles reported in Table 1. Conversely, the stronger cytostatic effect of CAI-conjugated particles on hypoxic MDA cells may result from a stronger inhibition of their extracellular carbonic anhydrases. Unlike HCT cells that express both CAIX and CAXII, MDA cells exhibit CAIX only,[78,85] which may contribute to this effect.

Our speculation was corroborated by the measurement of extracellular pH. This parameter was not affected by an addition of 2-methoxyethylamine-modified particles. Instead, according to Figure 4 (panel on the right), CAI-conjugated particles imparted a partial alkalinization of the extracellular pH of hypoxic cells only, which is ascribed to a specific inhibition of their CAIX or CAXII activity,[52,86] in line with the findings in standard solutions reported in Figure S1 of Supporting Information. This effect was much stronger on MDA than HCT cells, which correlates well with the cytostatic effect seen in the leftmost panels of Figure 4. In light of the particle uptake shown in Table 1, these results are attributed to a slower turnover of transmembrane CAs in MDA than HCT cells, which makes their saturation with CAIs to be more efficient.

2.5. Therapeutic Potential with an Optical Excitation

Figure 5 shows optical micrographs of HCT cells treated with different particles in normoxia or hypoxia and then excited with different optical power densities. These results are in line with the data reported in Table 1. Hypoxic cells incubated with CAI-conjugated particles were fully exterminated at power densities as low as 50 W cm^{-2}, which is almost in the same order as previous findings for gold nanorods targeted against more standard receptors, such as EGFR.[1,12] Conversely, normoxic cells exposed to CAI-conjugated particles started to undergo lethal damage around 120 W cm^{-2}, which was likely to originate from the residual nonspecific uptake seen by spectrophotometry. Instead, hypoxic cells treated with 2-methoxyethylamine-modified particles remained viable up to 150 W cm^{-2}. The contrast on MDA cells was more controversial, as it is expected from their poorer particle uptake (data not shown).

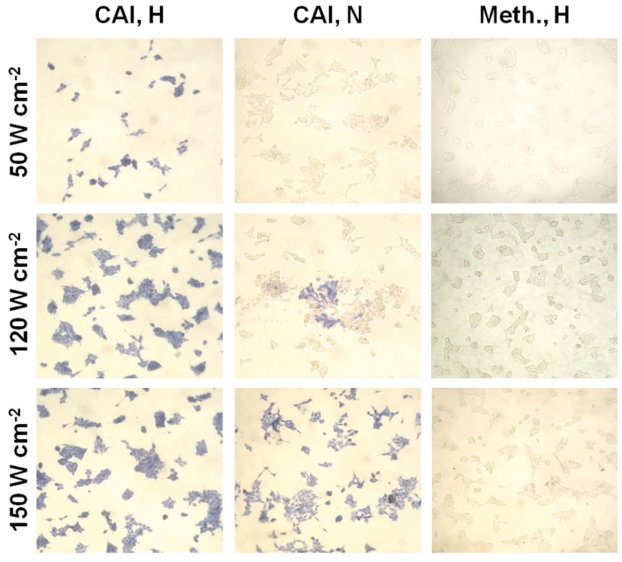

Figure 5. 470 μm × 400 μm optical micrographs of HCT cells treated with 100 μM Au particles with different terminations, i.e., CAIs or 2-methoxyethylamine (Meth.), and under different levels of oxygenation, i.e., hypoxia (H) or normoxia (N), and then excited with light at 810 nm and different power density for 5 min. After fixation, cells were stained with trypan blue.

2.6. Complementariness of Therapeutic Options

To our knowledge, this is the first example where the active targeting and cytotoxic activity of plasmonic particles is modulated with microenvironmental oxygenation, by the use of CAIs. These molecules serve both to impair the extracellular acidification necessary for tumor survival with an anaerobic glycolytic metabolism and as specific ligands for cancer recognition and optical sensitization with the plasmonic particles. In practice, those cells having a slower turnover of transmembrane CAs or CAIX only, as it may be the case of our MDA model, may suffer from the inhibitory power of our sulfonamide moieties even in the absence of an optical excitation, at the expense of a poor optical sensitization. We recall that, in this case, the role of the gold nanorods would be only that to impart impermeability to plasmatic membranes,[75,76] independent of their plasmonic features. Instead, those cells having a faster turnover of transmembrane CAs or also CAs other than CAIX, as it may be the case of our HCT model, may tolerate the presence of our particles in the absence of an optical excitation, while becoming an ideal target for the optical hyperthermia. The interplay of our twofold therapeutic option with the abundance of transmembrane CAs will be the subject of our future efforts.

We highlight that the pool of species available for CA inhibition is really broad,[72,73] which leaves significant opportunities for optimization in terms of efficiency and specificity. In addition, the use of these molecules holds a history of clinical experience[87] and the promise of cost effectiveness, which is another key advantage with respect to common ligands such as antibodies.

3. Conclusion

In conclusion, we have demonstrated a new concept to treat cancer with plasmonic particles such as gold nanorods by the addition of CAIs, which target hypoxic cells of common occurrence in a variety of solid tumors. The cellular uptake of our particles may be modulated with environmental oxygenation, thanks to the interplay of the impermeabilization to the cellular membranes imparted by the gold nanorods and the specificity for CAs provided by the CAIs. We tested the use of sulfonamides as an efficient model of CAIs. The introduction of these small molecules seems to outclass that of more conventional ligands, such as anti-CAIX antibodies, in terms of accumulation rates, possibly due to their better steric profiles. Our particles may offer complementary therapeutic opportunities, including an alkalinization of the cancer microenvironment, which frustrates the anaerobic metabolism needed for cellular survival under hypoxia,[50–53] thus exerting a cytostatic effect, and a sensitization to an optical ablation. We speculate that the hyperthermic option may remove possible drawbacks of a treatment of hypoxic tumors based on CAIs alone to lose efficiency in their normoxic periphery, simply by the modulation of heat diffusion.[88]

In the future, we wish to test the combination of gold nanorods with different formulations of CAIs, in order to really minimize nonspecific interactions with the cellular membranes and gain the slowest blood clearance. The next challenge will be to translate our results in vivo, in the presence of hypoxic tumors.

4. Experimental Section

Preparation and Characterization of CAI-Conjugated Gold Nanorods: All chemicals were purchased from Sigma Aldrich and used as received. Gold nanorods were synthesized by autocatalytic reduction of chloroauric acid by ascorbic acid in the presence of cetrimonium bromide, silver nitrate and ultra-small gold nanospheres, as it is described elsewhere.[77] Thereafter, particles were transferred at a concentration of 1.6 mM Au into a 100 mM acetate buffer at pH 5.0 and PEGylated by the addition of 50 μM heterobifunctional PEG strands with a mixture of 90% alpha mercapto omega methoxy and 10% alpha mercapto omega carboxy PEG (MW ≈ 5000 g mol^{-1}) (2 h at 37 °C). This mixture provides for excellent colloidal stability in biological buffers and ease to anchor desired amine-bearing species by amidation.[26] In detail, particles were transferred at a concentration of 1.6 mM Au into a 120 mM NaCl 10 mM MES buffer at pH 5.5 and activated by the addition of an equal volume of the same MES buffer containing 12 mM *N*-hydroxysuccinimide and 48 mM 1-ethyl-3-(3-dimethylaminopropyl) carbodiimide (15 min at 37°C). Finally, a double volume of the same MES buffer containing alternate amine-bearing species was added, in order to achieve their conjugation (1 h at 37 °C). Here, we dosed either of 2 mM 2-methoxyethylamine as a negative control that may restore the function of alpha mercapto omega methoxy PEG and minimize nonspecific interactions with plasmatic membranes,[20–22] 2 mM 4-(2-aminoethyl)benzenesulfonamide as a model of sulfonamide-bearing CAI, or 20 ppm of an antibody against CAIX as another positive control. In the latter instance, excessive succinimide-modified carboxy moieties were blocked by the addition of 1 mM 2-methoxyethylamine (30 min at 37 °C). All particles were purified by three cycles of centrifugation with a dead volume ratio of ≈ 1/200, transferred at a concentration of 4.0 mM Au into sterile PBS, stored at 4°C and used within one week of their preparation. Particles were characterized by the combination of a Philips CM12 (S)TEM transmission electron microscope, a Jasco V-560 spectrophotometer and a Malvern Nano ZS90 z scanner.

Preparation of Cellular Cultures and Measurement of Particle Cytotoxicity: Human HCT116 (ATCC, CCL-247) colon colorectal carcinoma and human MDA-MB-231 (ATCC, HTB-26) mammary adenocarcinoma cell lines were selected for their relevance in the literature on the expression of extracellular CAs under hypoxia.[51,89,90] Cells were cultured in a humidified incubator at 37°C in 5% CO_2 in DMEM medium supplemented with 10% FCS, 100 U/mL penicillin G and 100 μg/mL streptomycin and either incubated under normal conditions or exposed to hypoxia in a modulator incubator (1% O_2, 5% CO_2 and balanced N_2). Alternatively, hypoxic conditions were chemically induced under standard oxygenation by the use of a growth medium supplemented with 200 μM $CoCl_2$ as an hypoxia mimetic agent.[91] In order to investigate the cytotoxicity of our particles, we used an MTT assay. Cells were seeded and allowed to grow overnight. Particles were then added in different amounts and cells were incubated in standard conditions for 24 h. Care was taken to ensure that all cultures were subconfluent and contained similar densities of cells. The MTT reduction assay was performed as originally described by Mossman[92] and analyzed with a microplate reader from BMG Labtech. Data were expressed as percent of MTT reduction in treated with respect to untreated cells ($n = 9$).

Measurement of Particle Targeting In Vitro: The relative accumulation of particles in cells was visualized by silver enhancement[9,25] and quantified by a numerical model of their spectra of optical extinction. For the silver enhancement, cells were plated and allowed to grow overnight. Particles were then added in different amounts and cells were incubated in normoxia or hypoxia for 24 hours. Thereafter cells were fixed in 3.6% paraformaldehyde, rinsed with abundant water, stained by the addition of silver acetate and hydroquinone in a 12 mM citrate buffer at pH 3.8, rinsed with water after a few minutes (exactly the same time for

positive and negative samples in the same run) and inspected under a Leica Microsystems inverted phase-contrast microscope. For the optical measurements, 2×10^5 cells were plated into 25 cm flasks and allowed to recover and adhere to their bottom overnight. Then, appropriate amounts of particles were added and cells were incubated in normoxia or hypoxia for 24 h. Thereafter, cells were fixed, washed several times, reconstituted in 200 µL PBS in a quartz microcuvette and analyzed by a Jasco V-560 spectrophotometer. Their spectra of optical extinction were modeled as the sum of two contributions, that is, an empirical background from an unknown number of cells, which was calibrated in a preliminary measurement, plus a numerical approximation of the plasmonic band from an unknown number of gold nanorods. The latter was devised as a convolution integral between Gans lineshape[10,93,94] using the dielectric function of gold by Etchegoin et al.[95] and an unknown distribution of particle shapes. These statistics of particle shapes were retrieved for each sample de novo, in order to accommodate to possible variations of the plasmonic profiles of each sample. Details of this method are provided elsewhere.[93,94] Here, the exact conversion factor between the volume fraction of gold returned by the computation and the number density of particles was retrieved from a preliminary analysis of a standard suspension. With this factor, the output of this model conveys a quantitative rate of particles taken up per cell.

Measurement of Cellular Proliferation and Enzymatic Inhibition In Vitro: We addressed the therapeutic potential of our particles in the absence of an optical excitation, which may originate from the presence of CAIs. We contrasted the data from a time-lapse viability and proliferation analysis and the measurement of extracellular pH under hypoxia. For the time-lapse analysis, 2×10^5 cells were plated into 25 cm flasks and allowed to recover and adhere to their bottom overnight. Next day, 200 µM $CoCl_2$ and appropriate amounts of particles were added. Samples were video-recorded for 72 hours using a Zeiss inverted phase-contrast microscope. Viable cells were counted at 24, 48, and 72 h time points by three independent operators. The inhibition of the enzymatic activity of CAs and relevant changes in extracellular pH were assessed by the procedure in previous studies.[52,86] In brief, cells were plated and allowed to grow overnight. Particles were then added to a final concentration of 100 µM Au and cells were incubated in normoxia or hypoxia for 48 h. At that point, media were sampled and immediately probed with a Radiometer Analytical PHM210 digital pH-meter. Data from at least three independent experiments were expressed as the difference between the pH values measured in the samples treated with CAI- and 2-methoxyethylamine-conjugated particles (Δ pH).

Measurement of Optical Sensitization In Vitro: We investigated the therapeutic potential of our particles in combination with an optical excitation in vitro. For the stimulation of a hyperthermal damage, cells were plated and allowed to recover overnight. Particles were then added to a final concentration of 100 µM Au and cells were incubated in normoxia or hypoxia for 24 h. Then samples were irradiated with an El.En. Mod. WELD 800 low power diode laser with emission at 810 nm[78,88,93,94,96] for five minutes at different power densities. Samples were stained with trypan blue to reveal the distribution of dead cells as in a previous study,[96] fixed in 3.6% paraformaldehyde, washed in PBS and imaged under a Leica Microsystems inverted phase-contrast microscope.

Supporting Information

Supporting Information is available from the Wiley Online Library or from the author.

Acknowledgements

This work has been partially supported by the Project of the Health Board of the Tuscan Region "NANOTREAT".

Received: June 26, 2014
Revised: September 28, 2014
Published online: November 20, 2014

[1] X. Huang, I. H. El-Sayed, W. Qian, M. A. El-Sayed, *J. Am. Chem. Soc.* **2006**, *128*, 2115–2120.
[2] F. Ratto, P. Matteini, S. Centi, F. Rossi, P. Pini, *J. Biophotonics* **2011**, *4*, 64–73.
[3] E. C. Dreaden, A. M. Alkilany, X. Huang, C. J. Murphy, M. A. El-Sayed, *Chem. Soc. Rev.* **2012**, *41*, 2740–2779.
[4] J. K. Young, E. R. Figueroa, R. A. Drezek, *Ann. Biomed. Eng.* **2012**, *40*, 438–459.
[5] C. Kim, E. C. Cho, J. Y. Chen, K. H. Song, L. Au, C. Favazza, Q. A. Zhang, C. M. Cobley, F. Gao, Y. N. Xia, *ACS Nano* **2010**, *4*, 4559–4564.
[6] W. Lu, Q. Huang, G. Ku, X. Wen, M. Zhou, D. Guzatov, P. Brecht, R. Su, A. Oraevsky, L. V. Wang, C. Li, *Biomaterials* **2010**, *31*, 2617–2626.
[7] J. F. Lovell, C. S. Jin, E. Huynh, H. L. Jin, C. Kim, J. L. Rubinstein, W. C. W. Chan, W. G. Cao, L. V. Wang, G. Zheng, *Nat. Mater.* **2011**, *10*, 324–332.
[8] S. Manohar, C. Ungureanu, T. G. Van Leeuwen, *Contrast Media Mol. Imaging* **2011**, *6*, 389–400.
[9] E. B. Dickerson, E. C. Dreaden, X. Huang, I. H. El-Sayed, H. Chu, S. Pushpanketh, J. F. McDonald, M. A. El-Sayed, *Cancer Lett.* **2008**, *269*, 57–66.
[10] J. Pérez-Juste, I. Pastoriza-Santos, L. M. Liz-Marzán, P. Mulvaney, *Coord. Chem. Rev.* **2005**, *249*, 1870–1901.
[11] L. Tong, Q. S. Wei, A. Wei, J. X. Cheng, *Photochem. Photobiol.* **2009**, *85*, 21–32.
[12] C. Loo, A. Lowery, N. Halas, J. West, R. Drezek, *Nano Lett.* **2005**, *5*, 709–711.
[13] R. Bardhan, S. Lal, A. Joshi, N. Halas, *J. Acc. Chem. Res.* **2011**, *44*, 936–946.
[14] Y. Xia, W. Li, C. M. Cobley, J. Chen, X. Xia, Q. Zhang, M. Yang, E. C. Cho, P. K. Brown, *Acc. Chem. Res.* **2011**, *44*, 914–924.
[15] H. Stanwix, *Nanomedicine* **2013**, *8*, 9–11.
[16] R. G. Rayavarapu, W. Petersen, L. Hartsuiker, P. Chin, H. Janssen, F. W. B. van Leeuwen, C. Otto, S. Manohar, T. G. van Leeuwen, *Nanotechnology* **2010**, *21*, 145101.
[17] N. Khlebtsov, L. Dykman, *Chem. Soc. Rev.* **2011**, *40*, 1647–1671.
[18] A. M. Alkilany, L. B. Thompson, S. P. Boulos, P. N. Sisco, C. J. Murphy, *Adv. Drug Delivery Rev.* **2012**, *64*, 190–199.
[19] X. H. Huang, X. H. Peng, Y. Q. Wang, Y. X. Wang, D. M. Shin, M. A. El-Sayed, S. M. Nie, *ACS Nano* **2010**, *4*, 5887–5896.
[20] T. Niidome, M. Yamagata, Y. Okamoto, Y. Akiyama, H. Takahashi, T. Kawano, Y. Katayama, Y. J. Niidome, *J. Controlled Release* **2006**, *114*, 343–347.
[21] J. Lipka, M. Semmler-Behnke, R. A. Sperling, A. Wenk, S. Takenaka, C. Schleh, T. Kissel, W. J. Parak, W. G. Kreyling, *Biomaterials* **2010**, *31*, 6574–6581.
[22] F. Tatini, I. Landini, F. Scaletti, L. Massai, S. Centi, F. Ratto, S. Nobili, G. Romano, F. Fusi, L. Messori, E. Mini, R. Pini, *J. Mater. Chem. B* **2014**, *2*, 6072–6080.
[23] A. K. Iyer, G. Khaled, J. Fang, H. Maeda, *Drug Discovery Today* **2006**, *11*, 812–818.
[24] J. Y. Chen, D. L. Wang, J. F. Xi, L. Au, A. Siekkinen, A. Warsen, Z. Y. Li, H. Zhang, Y. N. Xia, X. D. Li, *Nano Lett.* **2007**, *7*, 1318–1322.
[25] M. Eghtedari, A. V. Liopo, J. A. Copland, A. A. Oraevsky, M. Motamedi, *Nano Lett.* **2009**, *9*, 287–291.
[26] C. Ungureanu, R. Kroes, W. Petersen, T. A. M. Groothuis, F. Ungureanu, H. Janssen, F. W. B. van Leeuwen, R. P. H. Kooyman, S. Manohar, T. G. van Leeuwen, *Nano Lett.* **2011**, *11*, 1887–1894.
[27] S. Kumar, J. Aaron, K. Sokolov, *Nat. Protoc.* **2008**, *3*, 314–320.
[28] C. Parolo, A. de la Escosura-Muñiz, E. Polo, V. Grazu, J. M. de la Fuente, A. Merkoçi, *ACS Appl. Mater. Interfaces* **2013**, *5*, 10753–10759.
[29] P. P. Joshi, S. J. Yoon, W. G. Hardin, S. Emelianov, K. V. Sokolov, *Bioconjug. Chem.* **2013**, *19*, 878–888.

[30] E. Lee, Y. Hong, J. Choi, S. Haam, J. S. Suh, Y. M. Huh, J. Yang, *Nanotechnology* **2012**, *23*, 465101.
[31] S. Charan, K. Sanjiv, N. Singh, F. C. Chien, Y. F. Chen, N. N. Nergui, S. H. Huang, C. W. Kuo, T. C. Lee, P. Chen, *Bioconjug. Chem.* **2012**, *23*, 2173–2782.
[32] J. Wang, K. Sefah, M. B. Altman, T. Chen, M. You, Z. Zhao, C. Z. Huang, W. Tan, *Chem. Asian. J.* **2013**, *10*, 2417–2422.
[33] J. Wang, G. Zhu, M. You, E. Song, M. I. Shukoor, K. Zhang, M. B. Altman, Y. Chen, Z. Zhu, C. Z. Huang, W. Tan, *ACS Nano* **2012**, *6*, 5070–5077.
[34] X. Yang, X. Liu, Z. Liu, F. Pu, J. Ren, X. Qu, *Adv. Mater.* **2012**, *24*, 2890–2895.
[35] Z. Heidari, R. Sariri, M. Salouti, *J. Photochem. Photobiol. B* **2013**, *130*, 40–46.
[36] M. Bartneck, T. Ritz, H. A. Keul, M. Wambach, J. Bornemann, U. Gbureck, J. Ehling, T. Lammers, F. Heymann, N. Gassler, T. Lüdde, C. Trautwein, J. Groll, F. Tacke, *ACS Nano* **2012**, *6*, 8767–8777.
[37] J. Wang, B. Dong, B. Chen, Z. Jiang, H. Song, *Dalton Trans.* **2012**, *41*, 11134–11144.
[38] W. Lu, G. D. Zhang, R. Zhang, L. G. Flores, Q. Huang, J. G. Gelovani, C. Li, *Cancer Res.* **2010**, *70*, 3177–3188.
[39] X. Yang, Z. Liu, Z. Li, F. Pu, J. Ren, X. Qu, *Chemistry* **2013**, *19*, 10388–10394.
[40] J. M. Saul, A. V. Annapragada, R. V. Bellamkonda, *J. Controlled Release* **2006**, *114*, 277–287.
[41] X. Ying, H. Wen, W. L. Lu, J. Du, J. Guo, W. Tian, Y. Men, Y. Zhang, R. J. Li, T. Y. Yang, D. W. Shang, J. N. Lou, L. R. Zhang, Q. Zhang, *J. Controlled Release* **2010**, *141*, 183–192.
[42] E. Kluza, D. W. J. van der Schaft, P. A. I. Hautvast, W. J. M. Mulder, K. H. Mayo, A. W. Griffioen, G. J. Strijkers, K. Nicolay, *Nano Lett.* **2010**, *10*, 52–58
[43] E. S. Day, L. N. Zhang, P. A. Thompson, J. A. Zawaski, C. C. Kaffes, M. W. Gaber, S. M. Blaney, J. L. West, *Nanomedicine* **2012**, *7*, 1133–1148.
[44] B. Brandt, S. Meyer-Staeckling, H. Schmidt, K. Agelopoulos, H. Buerger, *Clin. Cancer Res.* **2006**, *12*, 7252–7260.
[45] R. Li, H. Zhang, W. Yu, Y. Chen, B. Gui, J. Liang, Y. Wang, L. Sun, X. Yang, Y. Zhang, L. Shi, Y. Li, Y. Shang, *EMBO J.* **2009**, *28*, 2763–2776.
[46] P. Vaupel, *Oncologist* **2008**, *13*, 21–26.
[47] G. L. Semenza, *Trends Pharmacol. Sci.* **2012**, *33*, 207–214.
[48] B. Keith, M. C. Simon, *Cell* **2007**, *129*, 465–472.
[49] J. M. Heddleston, Z. Li, J. D. Lathia, S. Bao, A. B. Hjelmeland, J. N. Rich, *Br. J. Cancer* **2010**, *102*, 789–795.
[50] F. E. Lock, P. C. McDonald, Y. Lou, I. Serrano, S. C. Chafe, C. Ostlund, S. Aparicio, J.-Y. Winum, C. T. Supuran, S. Dedhar, *Oncogene* **2013**, *32*, 5210–5219.
[51] C. C. Wykoff, N. J. P. Beasley, P. H. Watson, K. J. Turner, J. Pastorek, A. Sibtain, G. D. Wilson, H. Turley, K. L. Talks, P. H. Maxwell, C. W. Pugh, P. J. Ratcliffe, A. L. Harris, *Cancer Res.* **2000**, *60*, 7075–7083.
[52] E. Svastova, A. Hulikova, M. Rafajova, M. Zat'ovicova, A. Gibadulinova, A. Casini, A. Cecchi, A. Scozzafava, C. T. Supuran, J. Pastorek, S. Pastorekova, *FEBS Lett.* **2004**, *577*, 439–445.
[53] S. K. Parks, J. Chiche, J. Pouysségur, *Nat. Rev. Cancer* **2013**, *13*, 611–23.
[54] D. Vullo, M. Franchi, E. Gallori, J. Pastorek, A. Scozzafava, S. Pastorekova, C. T. Supuran, *Bioorg. Med. Chem. Lett.* **2003**, *13*, 1005–1009.
[55] C. T. Supuran, *J. Enzyme Inhib. Med. Chem.* **2012**, *27*, 759–772.
[56] D. Vullo, A. Innocenti, I. Nishimori, J. Pastorek, A. Scozzafava, S. Pastoreková, C. T. Supuran, *Bioorg. Med. Chem. Lett.* **2005**, *15*, 963–969.
[57] D. Vullo, J. Voipio, A. Innocenti, C. Rivera, H. Ranki, A. Scozzafava, K. Kaila, C. T. Supuran, *Bioorg. Med. Chem. Lett.* **2005**, *15*, 971–976.
[58] C. T. Supuran, *J. Enzyme Inhib. Med. Chem.* **2013**, *28*, 229–230.
[59] C. T. Supuran, A. Maresca, F. Gregá , M. Remko, *J. Enzyme Inhib. Med. Chem.* **2013**, *28*, 289–293.
[60] A. Bonneau, A. Maresca, J.-Y. Winum, C. T. Supuran, *J. Enzyme Inhib. Med. Chem.* **2013**, *28*, 397–401.
[61] D. Neri, C. T. Supuran, *Nat. Rev. Drug Discovery* **2011**, *10*, 767–777.
[62] C. T. Supuran, *Nat. Rev. Drug Discovery* **2008**, *7*, 168–181.
[63] C. Ward, S. P. Langdon, P. Mullen, A. L. Harris, D. J. Harrison, C. T. Supuran, I. Kunkler, *Cancer Treatm. Rev.* **2013**, *39*, 171–179.
[64] A. Thiry, J. M. Dogné, B. Masereel, C. T. Supuran, *Trends Pharmacol Sci.* **2006**, *27*, 566–573.
[65] A. Kivela, S. Parkkila, J. Saarnio, T. J. Karttunen, J. Kivelä, A. K. Parkkila, A. Waheed, W. S. Sly, J. H. Grubb, G. Shah, O. Türeci, H. Rajaniemi, *Am. J. Pathol.* **2000**, *156*, 577–584.
[66] P. Hynninen, L. Vaskivuo, J. Saarnio, H. Haapasalo, J. Kivelä, S. Pastoreková, J. Pastorek, A. Waheed, W. S. Sly, U. Puistola, S. Parkkila, *Histopathology* **2006**, *49*, 594–602.
[67] J. Haapasalo, M. Hilvo, K. Nordfors, H. Haapasalo, S. Parkkila, A. Hyrskyluoto, I. Rantala, A. Waheed, W. S. Sly, S. Pastorekova, J. Pastorek, A. K. Parkkila, *Neuro Oncol.* **2008**, *10*, 131–138.
[68] M. I. Ilie, V. Hofman, C. Ortholan, R. E. Ammadi, C. Bonnetaud, K. Havet, N. Venissac, J. Mouroux, N. M. Mazure, J. Pouysségur, P. Hofman, *Int. J. Cancer.* **2011**, *128*, 1614–1623.
[69] C. T. Supuran, F. Briganti, S. Tilli, W. R. Chegwidden, A. Scozzafava, *Bioorg. Med. Chem.* **2001**, *3*, 703–714.
[70] G. De Simone, C. T. Supuran, *Biochim. Biophys. Acta* **2010**, *1804*, 404–409.
[71] S. Pastorekova, J. Zavada, *Cancer Therapy* **2004**, *2*, 245–262.
[72] P. C. McDonald, J. Y. Winum, C. T. Supuran, S. Dedhar, *Oncotarget* **2012**, *3*, 84–97.
[73] S. M. Monti, C. T. Supuran, G. De Simone, *Expert Opin. Ther. Targets* **2013**, *23*, 737–749.
[74] J. Y. Winum, A. Maresca, F. Carta, A. Scozzafava, C. T. Supuran, *Chem. Commun.* **2012**, *48*, 8177–8179.
[75] M. Stiti, A. Cecchi, M. Rami, M. Abdaoui, V. Barra-gan-Montero, A. Scozzafava, Y. Guari, J. Y. Winum, C. T. Supuran, *J. Am. Chem. Soc.* **2008**, *130*, 16130–16131.
[76] F. Bellissima, F. Carta, A. Innocenti, A. Scozzafava, P. Baglioni, C. T. Supuran, D. Berti, *Eur. Phys. J. E Soft Matter* **2013**, *36*, 48–57.
[77] F. Ratto, P. Matteini, F. Rossi, R. Pini, *J. Nanopart. Res.* **2010**, *12*, 2029–2036.
[78] P. Matteini, F. Ratto, F. Rossi, S. Centi, L. Dei, R. Pini, *Adv. Mater.* **2010**, *22*, 4313–4316.
[79] M. Mazzoni, F. Ratto, C. Fortunato, S. Centi, F. Tatini, R. Pini, *J. Phys. Chem. C* **2014**, *118*, 20018–20025.
[80] M. Das, L. Mordoukhovski, E. Kumacheva, *Adv. Mater.* **2008**, *20*, 2371–2375.
[81] A. C. Faure, S. Dufort, V. Josserand, P. Perriat, J. L. Coll, S. Roux, O. Tillement, *Small* **2009**, *5*, 2565–2575.
[82] H. Chen, H. Paholak, M. Ito, K. Sansanaphongpricha, W. Qian, Y. Che, D. Sun, *Nanotechnology* **2013**, *24*, 355101.
[83] Ž. Krpeti , P. Nativo, V. Sée, I. A. Prior, M. Brust, M. Volk, *Nano Lett.* **2010**, *10*, 4549–4554.
[84] J. D. Watkins, R. Lawrence, J. E. Taylor, S. D. Bull, G. W. Nelson, J. S. Foord, D. Wolverson, L. Rassaei, N. D. M. Evans, S. A. Gascon, F. Marken, *Phys. Chem. Chem. Phys.* **2010**, *12*, 4872–4878.
[85] Y. Li, C. Tu, H. Wang, D. N. Silverman, S. C. Frost, *J. Biol. Chem.* **2011**, *286*, 15789–157896.
[86] Y. Lou, P. C. McDonald, A. Oloumi, S. Chia, C. Ostlund, A. Ahmadi, A. Kyle, U. Auf dem Keller, S. Leung, D. Huntsman, B. Clarke, B. W. Sutherland, D. Waterhouse, M. Bally, C. Roskelley, C. M. Overall, A. Minchinton, F. Pacchiano, F. Carta, A. Scozzafava, N. Touisni, C. T. Supuran, S. Dedhar, *Cancer Res.* **2011**, *71*, 3364–3376.
[87] C. T. Supuran, *Expert Opin. Ther. Pat.* **2013**, *23*, 677–679.

[88] P. Matteini, F. Tatini, L. Luconi, F. Ratto, F. Rossi, G. Giambastiani, R. Pini, *Angew. Chem. Int. Ed.* **2013**, *52*, 5956–5960.
[89] Y. Li, H. Wang, E. Oosterwijk, C. Tu, K. T. Shiverick, D. N. Silverman, S. C. Frost, *Cancer Invest.* **2009**, *27*, 613–623.
[90] P. Swietach, S. Patiar, C. T. Supuran, A. L. Harris, R. D. Vaughan-Jones, *J. Biol. Chem.* **2009**, *284*, 20299–20310.
[91] T. Naves, S. Jawhari, M. O. Jauberteau, M. H. Ratinaud, M. Verdier, *Biochem. Pharmacol.* **2013**, *85*, 1153–1161.
[92] T. Mosmann, *J. Immunol. Methods* **1983**, *65*, 55–63.
[93] F. Ratto, P. Matteini, A. Cini, S. Centi, F. Rossi, F. Fusi, R. Pini, *J. Nanopart. Res.* **2011**, *13*, 4337–4348.
[94] P. Matteini, F. Ratto, F. Rossi, M. de Angelis, L. Cavigli, R. Pini, *J. Biophotonics* **2012**, *5*, 868–877.
[95] P. G. Etchegoin, E. C. Le Ru, M. Meyer, *J. Chem. Phys.* **2006**, *125*, 164705.
[96] P. Matteini, M. R. Martina, G. Giambastiani, F. Tatini, R. Cascella, F. Ratto, C. Cecchi, G. Caminati, L. Dei, R. Pini, *J. Mater. Chem. B* **2013**, *1*, 1096–1100.